Phase Analysis for Frequency Standards in the Microwave and Optical Domains

Michael Kazda, Vladislav Gerginov, Nils Huntemann, Burghard Lipphardt, and Stefan Weyers

Abstract—**Coherent manipulation of atomic states is a key concept in high-precision spectroscopy and used in atomic fountain clocks and a number of optical frequency standards. Operation of these standards can involve a number of cyclic switching processes, which may induce cycle-synchronous phase excursions of the interrogation signal and thus lead to shifts in the output of the frequency standard. We have built a field-programmable gate array (FPGA)-based phase analyzer to investigate these effects and conducted measurements on two kinds of frequency standards. For the caesium fountains PTB-CSF1 and PTB-CSF2, we were able to exclude phase variations of the microwave source at the level of a few microradians, corresponding to relative frequency shifts of less than 10^{-16}. In the optical domain, we investigated phase variations in PTB's Yb$^+$ optical frequency standard and made detailed measurements of acousto-optic modulator (AOM) chirps and their scaling with duty cycle and driving power. We ascertained that cycle-synchronous as well as long-term phase excursion do not cause frequency shifts larger than 10^{-18}.**

Index Terms—**Clocks, instrumentation and measurement, phase measurement, time measurement.**

I. INTRODUCTION

IN ATOMIC frequency standards, the utilization of separated oscillatory fields (Ramsey method) is well established because of its increased spectral resolution compared to the utilization of a single oscillatory field for the same interaction time and because of other advantages [1], [2]. However, the pulsed operation mode of fountain clocks and optical frequency standards involves a number of cyclic switching processes, which may cause cycle-synchronous phase changes of the oscillatory field during the Ramsey interaction and thereby induce shifts in the output frequency. In a fountain clock, the origin of detrimental cyclic phase excursions can be the utilization of an interferometric microwave switch [3], employed for switching off the microwave signal between the two subsequent atom–field interactions. Such cycle-synchronous phase variations at the few microradians level result in frequency shifts in the range of 10^{-16}, which is comparable to the level of the dominant uncertainty contributions in today's state-of-the-art atomic fountain clocks [4]–[8].

To detect small phase variations of the microwave field in fountain clocks, sophisticated phase-analyzing techniques have been developed [3], [9], [10], capable of coherent averaging synchronous to the fountain cycle. Based on these techniques we have developed a phase analyzer system utilizing a commercially available field-programmable gate array (FPGA) with an analog–digital converter front end. The data acquisition and filtering is entirely carried out within the FPGA, enabling the use of variable filters and decimation techniques as well as digital demodulation of the in-phase and quadrature (I/Q) signals and phase detection. Due to the large on-board memory, high-resolution measurements can be performed for long interrogation cycles. For our caesium fountain clocks, after 12 h of averaging, the analyzer allows for the detection of cycle-synchronous phase excursions that would cause frequency shifts of less than 10^{-16}.

The increased processing speed of our system enables likewise its application in optical frequency standards. In our single-ion optical frequency standard based on the $^2S_{1/2} \rightarrow {}^2F_{7/2}$ electric octupole transition of ^{171}Yb$^+$, a Ramsey-type excitation scheme is employed to avoid interaction-induced frequency shifts [11]. Because there is no active stabilization of the optical path length between the interrogation laser and the position of the ion in this frequency standard, cycle-synchronous phase excursions can lead to an error in the observed transition frequency. To investigate the magnitude of these phase excursions, we set up an interferometer and modified our phase analyzer for the analysis of the beat signals. After 24 h of data acquisition, we are able to determine phase excursions that correspond to frequency shifts of less than 10^{-18}.

In the following, we will first give an overview of the measurement system and the techniques common to both measurement cases in the microwave and optical domains. Then, we will explain the special requirements for measurements at the atomic fountain clocks and present results. The Yb$^+$-interrogation cycle will be introduced and the setup required for optical phase measurements will be defined. With this setup, we measured the phase excursion due to cyclic changes in the power of the signal that drives an acousto-optic modulator (AOM), known as the AOM chirp.

II. DESIGN

In cyclic processes, signal transients buried deeply in uncorrelated noise can be recovered by averaging data point-by-point over multiple cycles. Noise components of the signal are attenuated in relation to the number of averages. This technique is known as coherent averaging. To investigate possible phase
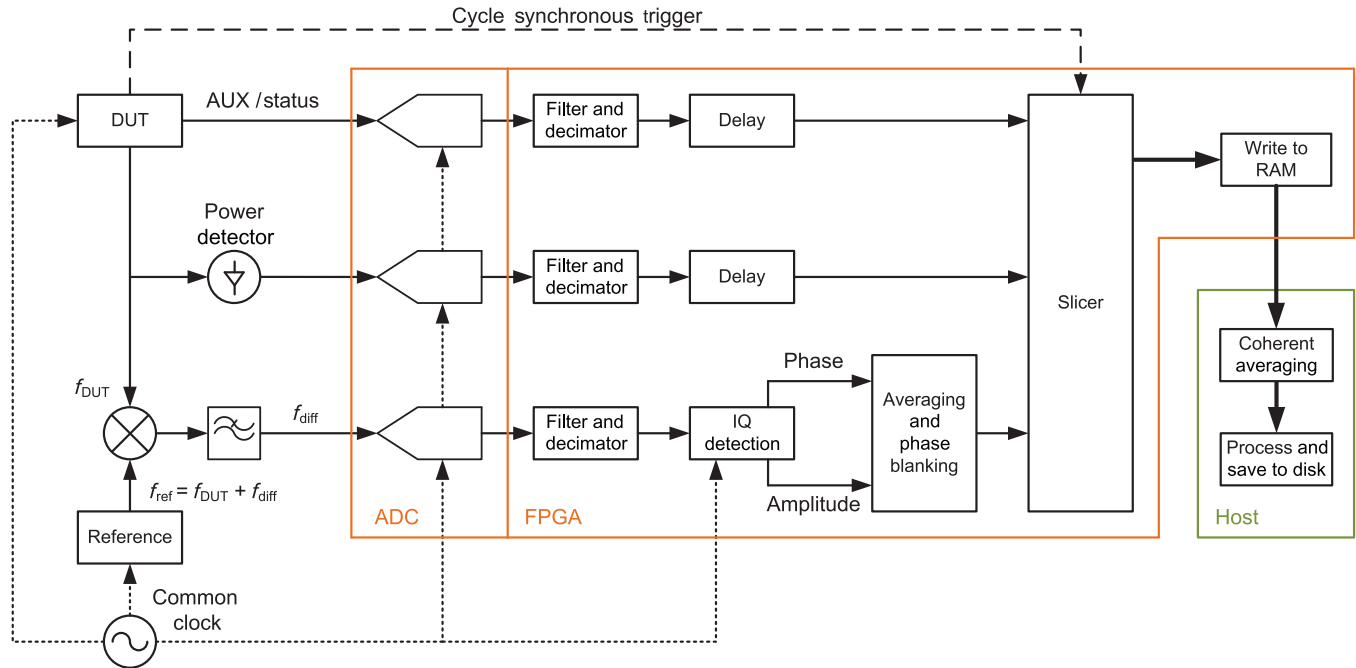
Fig. 1. Analyzer setup consisting of analog front end, AD-converter, and digital data processing.

transients in our atomic frequency standards, we have built an analyzer (Fig. 1) based on this averaging technique. It supports variable analysis bandwidths and cycle lengths up to several seconds with a maximum time resolution of $1\,\mu s$. Possible sources of phase variations, e.g., temperature changes, can be correlated by using two additional channels that are aligned with the averaged phase data.

Since the frequencies f_{DUT} of the devices under test (DUT) investigated here are outside the limited bandwidth of the system, they are downmixed to a frequency f_{diff}. A reference synthesizer is used to generate the required frequency $f_{\text{ref}} = f_{\text{DUT}} + f_{\text{diff}}$. After downmixing, the signal is fed to an antialiasing filter and then AD-converted with sample rate of 120 MS/s. Once the signal is digitized, all data processing is performed in the FPGA. First, the signal is filtered and decimated [12]. This stage allows for variable decimation factors, depending on the required time resolution. The time resolution, decimation factor and difference frequency f_{diff} are chosen according to specific requirements. The decimated signal is fed to an IQ-detector algorithm, where a direct digital synthesis (DDS) is implemented in software to generate a sinusoidal signal and the corresponding quadrature signal. Both signals are mixed with the decimated signal and phase and amplitude are calculated. Depending on the application, phase variations larger than 2π during one measurement cycle are possible. We, therefore, need to implement a phase-unwrapping algorithm in a later stage. However, when the signal level from the DUT is too low, the IQ-detector will give almost random phase values, which cannot be processed reliably by an unwrapping algorithm. Therefore, the amplitude information is used to mark phase values as valid or invalid. The output of this averaging and phase-blanking block is a continuous data stream.

To facilitate coherent averaging, the stream has to be divided in packages synchronous to the DUT cycle. A cycle-synchronous trigger is fed to a digital input of the FPGA

and the data stream is divided into evenly sized packages. In the slicer, the data points get time stamps relative to the cycle-synchronous trigger. Therefore, no delays are introduced due to further postprocessing. These data packages are written to RAM connected directly to the FPGA. The host monitors the acquisition and reads completed slices into the host memory, where they are coherently averaged. It also performs phase-unwrapping, various statistical calculations, and consistency checks. The averaged data as well as statistics are then saved to disk.

Parallel to the phase detection, the power level of the DUT and temperature or status information from the DUT are monitored. These signals are AD-converted, filtered, and decimated, similar to the phase signal. To compensate for delays in the IQ-demodulation of the phase signal, a small delay needs to be inserted. The phase stream and the other data streams are now aligned and can be averaged.

The analyzer is conceived for detecting periodic phase perturbations. A common clock is employed to ensure a stable phase relation between the analog signals and the digital detection and demodulation stages. For data acquisition and processing, a PXI System from National Instruments in combination with a 7966R FPGA card and a 5734R ADC converter front end is used. National Instruments Labview was used to program the FPGA as well as the host software.

Several tests were conducted to ensure proper operation of the analyzer, similar to [9]. For example, we slightly detuned the frequency of the analyzer by 0.1 µHz, and after 100 000 measurement cycles, we were able to observe a consistent linear phase ramp of 0.2π µrad over 1 s.

III. INVESTIGATION OF THE CAESIUM FOUNTAIN

Atomic fountain clocks use the Ramsey interrogation method to provide a realization of the SI second [13]. They employ
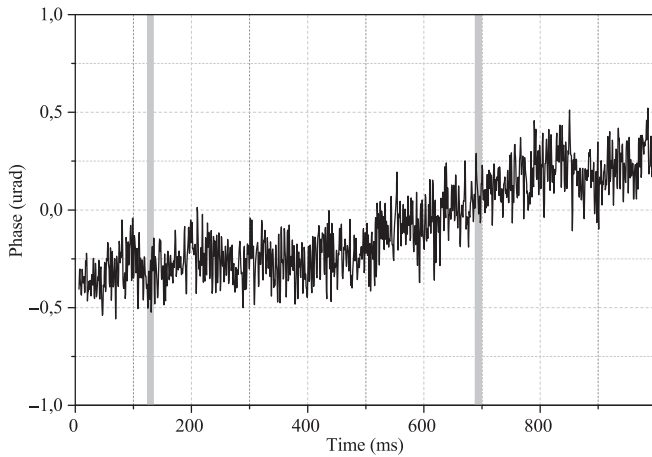
Fig. 2. Phase measurement of the microwave interrogation signal of CSF1 averaged over 60 000 cycles. The two Ramsey interactions are marked by the gray-shaded stripes. The standard deviation calculated from the independently characterized DUT noise of 0.2 μrad is in good agreement with the standard deviation of the measured phase values. Note that there is a gap in the data of 115 ms between the end and the beginning of the depicted data set.

a cyclic process, consisting of multiple stages. In a caesium fountain, the atoms are first cooled in the intersection region of six laser beams and subsequently launched vertically by laser frequency detuning. After launching, all laser beams are switched off and the cloud follows a ballistic trajectory. In a state-selection microwave cavity, the atoms are prepared in a single hyperfine magnetic substate, before on the way up and on the way down the atoms pass through the Ramsey cavity where they interact with the microwave field. After the second cavity passage, detection lasers probe the atom state population. At each cycle, the frequency of the microwave field in the Ramsey cavity is detuned to probe the transition probabilities at both sides of the central Ramsey fringe alternately. The resulting discriminator signal is used by a computer to control the output frequency f_{DUT} of the microwave synthesizer.

Because of the resulting cyclic changes of f_{DUT}, the reference frequency f_{ref} for the phase analyzer (Fig. 1) needs to be adjusted accordingly to ensure f_{diff} to be constant at 10 kHz. The required measurement time to evaluate phase excursions is significantly reduced by referencing the microwave synthesizer of the fountain to an optically stabilized 9.6-GHz oscillator [14], [15]. Its phase noise has been characterized in [15]. We can estimate the phase noise to be about 50 μrad rms (single cycle) within a bandwidth of 1–400 Hz. This oscillator is used as the common clock and divided down to 10 MHz to lock the FPGA and ADC clocks.

With this analyzer, we conducted phase measurements for our fountains CSF1 [16], [17] and CSF2 [18]. In Fig. 2, a phase measurement of the Ramsey interrogation signal of PTB's fountain clock CSF1 is shown with a time resolution of 0.5 ms. This measurement was performed in an operational mode, in which all signals and switching processes were applied as in the normal frequency measurement mode of CSF1, except the Ramsey output signal of the 9.192-GHz synthesis which was connected to the phase analyzer. The data are averaged for about 18 h, corresponding to 60 000 fountain cycles. The two gray-shaded stripes mark the occurrence of the two successive

Ramsey interactions, each with a duration of about 10 ms. From the data in Fig. 2, we estimate the phase difference between the two interactions to be smaller than 0.5 μrad, corresponding to a frequency shift of less than 2×10^{-17}. The standard deviation of the data set is 0.25 μrad. Similar results have been obtained for CSF2.

IV. INVESTIGATION OF THE YB+ OPTICAL FREQUENCY STANDARD

At PTB, we are currently investigating optical frequency standards based on the $^{171}Yb^+$ quadrupole and octupole transitions [15], [19]. For the octupole transition, we employ the hyper-Ramsey-scheme (HRS) [2], [11]. In this scheme, phase and frequency steps are applied to the interrogation laser light via an AOM controlled by a DDS. Changes in the power of the signal that drives the modulator lead to temperature changes of its crystal and in turn change the corresponding optical path length due to thermal expansion and the temperature dependence of the refractive index. The magnitude of the so-called AOM chirp depends on the power and the duty cycle of the driving signal [20], [21]. To reduce this effect, mechanical shutters are used to block the light during dark times and the AOM driving power is only switched off for short intervals in order to define the edges of the Ramsey pulses and during phase changes of the DDS.

In contrast to optical lattice clocks, where the realization of a path length stabilization between probe laser and the position of the atoms is straightforward [22], for our setup no active path length stabilization is implemented for the free-space probe laser beam so far. Residual phase fluctuations and drifts can therefore introduce frequency shifts. These can result not only from the aforementioned AOM chirps but also from air turbulences or thermal effects in optical parts or the mechanical setup. However, effects that are synchronous with the interrogation cycle require particularly careful consideration.

To evaluate such shift effects for the optical frequency standard, we need to determine the phase of the laser light after passage through the AOM and free-space propagation by setting up an interferometer (see Fig. 3). In the long arm of the interferometer, the light is diffracted by a TeO₂-AOM, and a small fraction of the laser light is used to detect the optical power. By beating the light from the long arm against the light from the short reference arm, we detect the optical phase.

A 76-MHz signal generated by a DDS is used to drive the AOM, resulting in a 76-MHz beat note on the photo-detector (f_{DUT}). This beat note is amplified and mixed with 79 MHz generated by a second DDS. The resulting 3-MHz signal (f_{diff}) is fed directly to the phase analyzer. To correct for phase drifts and excursions resulting from the DDS that drives the AOM, we measured the 76-MHz DDS signal directly and subtracted the obtained phase data from the beat note measurements. Thermally induced phase changes in the photo-detector used for beat detection are not corrected for in the results presented here.

In contrast to the standard Ramsey method mentioned earlier, the HRS contains an additional pulse between the two Ramsey interactions [2], [11]. The particular scheme investigated here
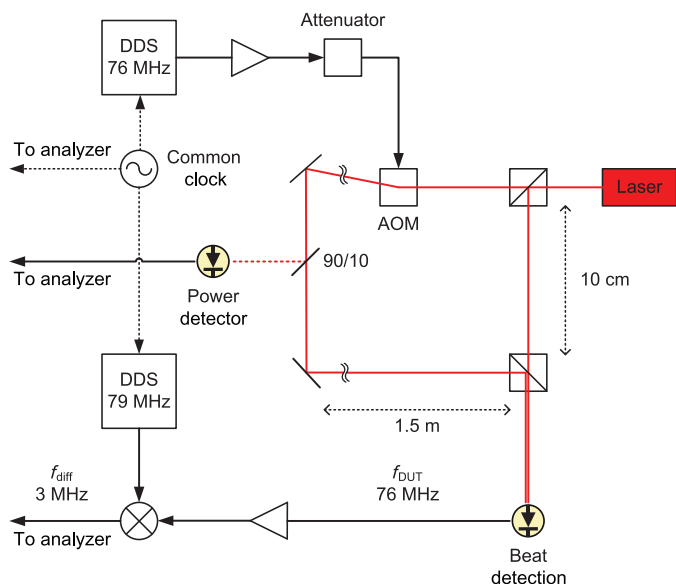
Fig. 3. Interferometric phase analysis setup at the Yb^+ optical frequency standard. For details see text. The setup is simplified, e.g., isolators and clock laser details are omitted.
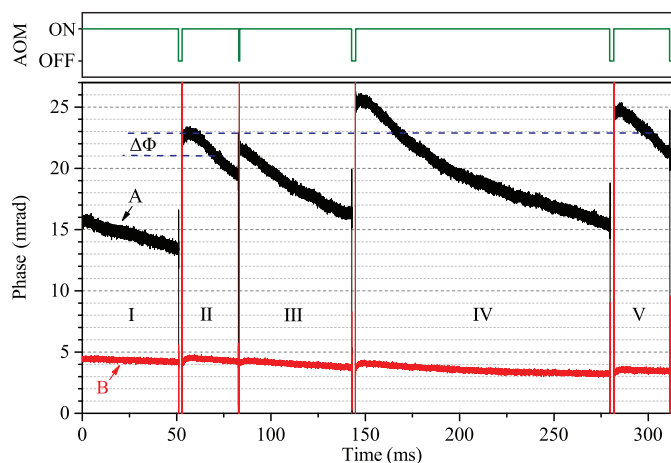

Fig. 4. Optical phase excursions averaged over repeated measurement cycles. The black curve (A) was acquired for an AOM driving power of 1 W; for the red curve (B), the nominal driving power of 50 mW was used. As illustrated in the upper part of this figure, the AOM is switched off for either 0.5 or 2 ms. Roman numerals mark the different phases of the interrogation cycle (see text). The observed phase difference $\Delta\Phi = 2$ mrad between the two Ramsey interactions in phases II and V is attributed to underlying long-term thermal drifts of the interferometer setup and should, therefore, be independent of the AOM driving power. Note that there is a gap in the data of about 50 ms between phases V and I.

consists of five phases, separated by short AOM off gaps with a duration of 2 or 0.5 ms as illustrated in Fig. 4. In phase I, readout and state preparation are performed and phases II and V are the actual Ramsey interactions. The additional pulse occurs in phase III and phase IV indicates the free precession time.

After sufficient cycle-synchronous averaging, various mechanisms affecting the phase can be identified, among them particularly AOM chirps. To accentuate their impact, we measured the phase excursions with an increased driving power of 1 W and for comparison under normal conditions with a driving power of 50 mW (A and B in Fig. 4). Distinctive phase

jumps during the off gaps can be traced back to the AOM crystal cooling down. Their magnitude depends on the AOM driving power and the switch-off time. At high driving power, these phase jumps are 9 and 2 mrad for off-times of 2 and 0.5 ms, respectively. Under normal operating conditions with low driving power, the phase jumps are largely reduced and smaller than 0.2 mrad. When switched back on, the AOM heats up toward the steady-state condition. This leads to phase drifts during the different stages of the scheme that can be translated into frequency offsets. The phase gradient during each of the two Ramsey interactions translates into an effective frequency detuning of about 20 mHz for high driving power and less than 2 mHz for low driving power.

In addition to these AOM chirps, Fig. 4 reveals an additional underlying phase drift, readily observed as the difference between the average phases of the Ramsey pulses II and V. This can be attributed to remaining thermal instabilities of the optical setup caused by periodic variations of the temperature in our air-conditioned laboratory of about 0.2 K over 5000 s. The mean temperature, however, is long-term stable to better than 0.1 K, so that the observed phase drift should average out, if the measurement time is significantly larger than the time scale of temperature fluctuations. For the black curve, 100 000 cycles were averaged. The difference of the mean phases in the two Ramsey interactions $\Delta\Phi = 2$ mrad is clearly visible. For the red curve, 230 000 cycles were averaged and the phase difference is reduced to 1 mrad. This phase difference corresponds to a relative frequency shift of about 1×10^{-18} that is significantly smaller than the instability of the frequency standard at the chosen measurement time of 1 day.

V. CONCLUSION AND OUTLOOK

We successfully implemented a phase analyzer for detecting cycle-synchronous phase excursions and illustrated two applications for frequency standards in the microwave and optical domains. We were able to prove that no significant uncertainty contribution in our caesium fountains is to be expected from phase variations of the microwave source when a continuous microwave signal is used. In the next step we will use the analyzer to validate our interferometric microwave switch for regular use.

In the optical domain, we measured AOM chirps and their scaling with duty cycle and driving power with high phase resolution and investigated long-term thermal drift effects of PTB's Yb^+ optical frequency standard setup. Since the phase analyzer provides high time resolution, we plan to investigate the effects of short-term phase fluctuations on the transition frequency.

REFERENCES

[1] N. F. Ramsey, "Experiments with separated oscillatory fields and hydrogen masers," *Rev. Mod. Phys.*, vol. 62, pp. 541–552, Jul. 1990.

[2] V. I. Yudin, "Hyper-Ramsey spectroscopy of optical clock transitions," *Phys. Rev. A*, vol. 82, no. 1, p. 011804, 2010.

[3] G. Santarelli *et al.*, "Switching atomic fountain clock microwave interrogation signal and high-resolution phase measurements," *IEEE Trans. Ferroelectr. Freq. Control*, vol. 56, no. 7, pp. 1319–1326, Jul. 2009.

[4] S. Weyers, V. Gerginov, N. Nemitz, R. Li, and K. Gibble, "Distributed cavity phase frequency shifts of the caesium fountain PTB-CSF2," *Metrologia*, vol. 49, no. 1, pp. 82–87, 2012.

[5] J. Guena *et al.*, "Progress in atomic fountains at LNE-SYRTE," *IEEE Trans. Ultrason. Ferroelectr. Freq. Control*, vol. 59, no. 3, pp. 391–409, Mar. 2012.

[6] R. Li, K. Gibble, and K. Szymaniec, "Improved accuracy of the NPL-CsF2 primary frequency standard: Evaluation of distributed cavity phase and microwave lensing frequency shifts," *Metrologia*, vol. 48, no. 5, pp. 283–289, 2011.

[7] T. P. Heavner *et al.*, "First accuracy evaluation of NIST-F2," *Metrologia*, vol. 51, no. 3, p. 174, 2014.

[8] F. Levi, D. Calonico, C. E. Calosso, A. Godone, S. Micalizio, and G. A. Costanzo, "Accuracy evaluation of ITCsF2: A nitrogen cooled caesium fountain," *Metrologia*, vol. 51, no. 3, p. 270, 2014.

[9] G. Santarelli *et al.*, "Phase transient measurement at the micro radian level for atomic fountain clocks," in *Proc. 20th Eur. Freq. Time Forum (EFTF)*, Mar. 2006, pp. 166–172.

[10] Y. Zhang, K. Liu, F. Fang, N. Liu, and T. Li, "Thermal effect of the microwave Mach-Zehnder interferometric switch," in *Proc. IEEE Int. Freq. Control Symp. (FCS)*, May 2014, pp. 1–3.

[11] N. Huntemann *et al.*, "Generalized Ramsey excitation scheme with suppressed light shift," *Phys. Rev. Lett.*, vol. 109, p. 213002, 2012.

[12] R. E. Crochiere and L. Rabiner, "Optimum FIR digital filter implementations for decimation, interpolation, and narrow-band filtering," *IEEE Trans. Acoust. Speech Signal Process.*, vol. SP-23, no. 5, pp. 444–456, Oct. 1975.

[13] R. Wynands and S. Weyers, "Atomic fountain clocks," *Metrologia*, vol. 42, no. 3, pp. 64–79, 2005.

[14] S. Weyers, B. Lipphardt, and H. Schnatz, "Reaching the quantum limit in a fountain clock using a microwave oscillator phase locked to an ultrastable laser," *Phys. Rev. A*, vol. 79, no. 3, p. 031803, 2009.

[15] C. Tamm *et al.*, "Cs-based optical frequency measurement using cross-linked optical and microwave oscillators," *Phys. Rev. A*, vol. 89, p. 023820, Feb. 2014.

[16] S. Weyers, U. Hübner, R. Schröder, C. Tamm, and A. Bauch, "Uncertainty evaluation of the atomic caesium fountain CSF1 of the PTB," *Metrologia*, vol. 38, no. 4, pp. 343–352, 2001.

[17] S. Weyers, A. Bauch, R. Schröder, and C. Tamm, "The atomic caesium fountain CSF1 of PTB," in *Proc. 6th Symp. Freq. Stand. Metrol.*, 2001, pp. 64–71.

[18] V. Gerginov, N. Nemitz, S. Weyers, R. Schröder, D. Griebsch, and R. Wynands, "Uncertainty evaluation of the caesium fountain clock PTB-CSF2," *Metrologia*, vol. 47, no. 1, pp. 65–79, 2010.

[19] N. Huntemann, M. Okhapkin, B. Lipphardt, S. Weyers, C. Tamm, and E. Peik, "High-accuracy optical clock based on the octupole transition in $^{171}Yb^+$," *Phys. Rev. Lett.*, vol. 108, p. 090801, Feb. 2012.

[20] C. Degenhardt, T. Nazarova, C. Lisdat, H. Stoehr, U. Sterr, and F. Riehle, "Influence of chirped excitation pulses in an optical clock with ultracold calcium atoms," *IEEE Trans. Instrum. Meas.*, vol. 54, no. 2, pp. 771–775, Apr. 2005.

[21] T. Rosenband *et al.*, "Frequency ratio of Al$^+$ and Hg$^+$ single-ion optical clocks; Metrology at the 17th decimal place," *Science*, vol. 319, no. 5871, pp. 1808–1812, 2008.

[22] S. Falke, M. Misera, U. Sterr, and C. Lisdat, "Delivering pulsed and phase stable light to atoms of an optical clock," *Appl. Phys. B*, vol. 107, no. 2, pp. 301–311, 2012.

Authors' photographs and biographies not available at the time of publication.